Comprehensive molecular level characterization of protein- and polyphenol-rich tara (*Caesalpinia spinosa*) seed germ flour suggests novel hypothesis about possible accidental hazards

Olga Fierro [a,1], Francesco Siano [a,1], Mariacristina Bianco [b], Ermanno Vasca [b], Gianluca Picariello [a,*]

[a] *Istituto di Scienze dell'Alimentazione, Consiglio Nazionale delle Ricerche, Via Roma 64, 83100 Avellino, Italy*
[b] *Dipartimento di Chimica e Biologia "A. Zambelli", Università degli Studi di Salerno, Via Giovanni Paolo II 132, 84084 Fisciano (SA), Italy*

ARTICLE INFO

ABSTRACT

Tara (*Caesalpinia spinosa*, *Leguminosae*) seed germ (TSG), a by-product of tara gum (E417) extraction, has been used as a protein- and polyphenol-rich food ingredient for human and animal nutrition. Nevertheless, TSG is the alleged culprit for a recent foodborne outbreak of even severe acute illnesses that have affected hundreds of individuals in the USA, perhaps triggered by nonprotein amino acids such as baikiain. Herein, the composition of TSG has been characterized at molecular level, with a focus on proteins, phenolics, lipids, and mineral composition. TSG contains 43.4 % (w/w) proteins, tentatively identified for the first time by proteomics, and 14 % lipids, consisting of 83.6 % unsaturated fatty acids, especially linoleic acid. Ash is surprising high (6.5 %) because of an elevated concentration of P, K, Ca, and Mg. The detection of a rare earth element such as gadolinium (Gd, 1.6 mg kg^{-1}), likely sourced from anthropogenic pollution, suggests alternative hypotheses for the origin of TSG hazards.

1. Introduction

Caesalpinia spinosa, commonly referred to as tara or Peruvian carob, is a small thorny shrub or small tree (2 to 3 m in height) belonging to *Leguminosae*, with spreading, gray barked leafy branches, large yellow to orange color flowers and green, reddish and light to dark brown color fruits, constituted by approximately 65 % (w/w) dry and indehiscent pods and 35 % (w/w) brown, ovate, smooth and very hard seeds. The name "tara", which in the Aymara language means "flat", is due to its flat-shaped fruits (pods with seeds) (Desai, Prajati, & Chandarana, 2022).

Tara tree is native to the Cordillera region of Bolivia, Peru, and northern Chile, where it grows wildly at 1000–3000 m altitudes above ocean level and thrives in arid or semi-desert soils (Glicksman, 1986). However, tara tree also grows in other South American countries as well as in North Africa (mainly Morocco), East Africa, and some Chinese provinces (Wu, Ding, Jia, & He, 2015; Hidalgo et al., 2020).

C. spinosa is also known as an ornamental plant, and from an ecological point of view the value of tara trees lies in their capacity to intercept fog droplets, increasing the water input into the environment (Balaguer et al., 2011). Since ancient times, tara has been highly appreciated for multiple purposes: pre-Incacivilizations used the fruits of the tree (known as "Incas' green gold") to produce dyes for textiles and ceramics, and tannins for leather and medicines. Gallotannins of tara pods are still used for leather tanning, in the production of plastics and adhesives, as wine clarifiers, malt substitutes, and antioxidants for the oil industry (Abd Alla, Sen, & El-Naggar, 2012; Chambi et al., 2013). Several interesting food applications that exploit the antioxidant capacity of extracts from tara pods have been recently described (Pedreschi et al., 2018; Pedreschi et al., 2022; Campos et al., 2024). Currently, tara is mainly cultivate for the gum, which is a galactomannan soluble in hot water and partly soluble in cold water constituting nearly the entire seed endosperm. It is extracted and purified as a white-pale yellow powder and finds application as a food packaging film and as a pharmaceutical or cosmetic excipient because of its biodegradability and biocompatibility (Chi et al., 2018; Ma, Ren, & Wang, 2017). Similar to locust bean gum (E410), which is obtained from carob (*Ceratonia siliqua*) seed endosperm, tara gum is primarily a food additive (E417) in high

demand by the food industry for its properties as a binder, thickener, moisture retainer, emulsifier and stabilizer (Mukherjee et al., 2023). Tara gum improves texture and prevents phase separation in dairy products such as ice creams, yogurt, and cheese, or in sauces, fruit juices, smoothies, and protein shakes. It also enhances dough elasticity, thereby increasing the volume of baked items (Gelling, 2019). The use of tara gum as a food additive has been authorized in the European Union by Regulation (EC) No 1333/2008 (Regulation EC, 2008). In a more recent re-evaluation of its safety profile, the EFSA (European Food Safety Agency) panel on food additives has excluded concerns for humans associated with the consumption of even large quantities of tara gum (EFSA Panel on Food Additives and Nutrient Sources added to Food (ANS). Re-evaluation of tara gum (E 417) as a food additive. (2017), 2017), based on the outcomes of long-term *in vivo* assessments (Borzelleca, Ladu, Senti, & Egle, 1993).

Tara derivatives have an annual global demand of around 42,300 tons, which corresponds to nearly 80,000 tons of pods (Chambi et al., 2013). However, because of its excellent technological properties, the industrial demand for tara galactomannans is sharply growing. Peru dominates the market of these products with 85 % of the world exports (Santos, Dos Santos, de Carvalho, de Carvalho, & Garcia-Rojas, 2019).

Despite a certain intra-species variability, tara seeds consist of 38–40 % husk, 30–34 % endosperm, and 27–30 % germ (Borzelleca et al., 1993). To remove the seed coat while preserving the integrity of the endosperm, seeds alternatively undergo treatments with mineral acids or roasting processes (Cruz Alcedo, 1999; Desai et al., 2022).

Regardless of the gum extraction process, tara seed germ (TSG) is sifted as an intensely yellow-coloured powder, whose pigments are alcohol soluble, suggesting the presence in large amounts of phenolic compounds structurally related to those occurring also in the seed germ of several *Leguminosae* as well as in wheat (*Triticum* spp.) germ (Geng et al., 2016). Indeed, *C. siliqua* and *Prosopis* spp. germ contains relatively abundant *C*-glycoside derivatives of apigenin (Picariello et al., 2017), which exhibit antioxidant, anti-inflammatory, hepatoprotective, and anticancer activity (Bucar, Xiao, & Ochensberger, 2021), and are inhibitors of pancreatic α-amylase and intestinal α-glycosidases with hypoglycemic potential (Siano et al., 2023a). Despite the considerable commercial value of the endosperm, the germ is a by-product only partly used for livestock feed, and implies disposal costs. Yet TSG flour is a very interesting food ingredient from functional and nutritional standpoints, by virtue of the high protein content and the presumed presence of bioactive phenol compounds.

However, the safety profile of TSG has been recently questioned. In fact, TSG flour is the alleged causative agent of an outbreak involving 393 individuals in the USA who experienced from mild to severe and debilitating hepatotoxic effects. This circumstance led Daily Harvest Co. (New York, USA) to issue a voluntary recall of TSG flour-containing newly launched French Lentil & Leek Crumbles. Concomitantly, some big producers have precautionarily removed TSG from the ingredient list of protein-enriched foods and beverages, such as the "superfood" smoothies, pending a definitive ruling from the Food and Drug Administration. While no unequivocal evidence has emerged from extensive toxicological tests, the possible cause of the intoxication has recently been attributed to *in vivo* metabolites of nonprotein amino acids, such as baikiain, occurring at high levels in TSG (Chittiboyina et al., 2023). The mechanism underlying the pathological response might involve only a cohort of genetically predisposed individuals like for favism. One of the supposed harmful baikiain metabolites is its product of water addition to a carbon double bond, namely 4-hydroxypipecolic acid. However, this latter amino acid occurs at discrete amount in *C. siliqua* germ flour (Grobbelaar, Pollard, & Steward, 1955), which has never raised safety concerns despite its rather extensive use for human consumption. Clearly, this information is not conclusive because the absorption and post-ingestion metabolism of baikiain and 4-hydroxypipecolic acid might be different, but it underlines the need to define the toxicity profile of these non-protein amino acids.

Anyway, the information available on the TSG composition remains scarce and fragmentary since it is based on a few rather dated studies (Re-Jiménez & Amadò, 1989; Borzelleca et al., 1993).

In the perspective of re-using an agro-industrial by-product with potential nutritional and functional benefits and speculating about the presence of possible harmful components, this work reports on an accurate characterization of the TSG at the molecular level, with special emphasis on proteins, phenol compounds, lipids, and mineral composition.

2. Materials and methods

2.1. Tara germ flour

Tara seed germ (TSG) flour was a gentle gift from Silvateam SpA (San Michele Mondovì, Cuneo, Italy), which is one of the largest companies committed in the commercialization of Peruvian tara products. Tara trees were grown in the Huánuco district, Peru, and pods were collected in 2023. The germ flour results as a by-product from the gum extraction from the seeds. TSG flour was received vacuum packed in a refrigerated box and was stored at −26 °C until analysis. Carob (*Ceratonia siliqua*) germ flour, used as a reference sample in this study, was a kind gift from Carob Ingredients Co., Casablanca, Morocco (https://www.carobingredients.com) (Siano et al., 2023a).

2.2. Chemicals

All chemicals used in this work were purchased from Merck-Sigma-Aldrich (St. Luis, Mo, USA), except for nitric acid 65 % (v/v), sulphuric acid 96 % (v/v) and HPLC-MS grade water that were from Carlo Erba Reagents (Milan, Italy). Reagents for electrophoresis analysis were from Bio-Rad (Milan, Italy).

2.3. Attenuated total reflectance-Fourier transform infrared (ATR-FTIR) spectroscopy

ATR-FTIR analyses were performed using a Spectrum 400 spectrophotometer (PerkinElmer, Waltham, MA, USA), equipped with a deuterated triglycine sulfate (DTGS) detector. Flour samples were analyzed without any previous treatment. Spectra were recorded in the 650–4000 cm^{-1} region at 32 scans/spectrum range and with resolution of 4 cm^{-1}. Analyses were performed in triplicate and the average spectra were processed using the PE Spectrum software (version 10.5.1) from PerkinElmer. ATR-FTIR was also used for quantifying phospholipids in the lipid fraction, according to a previously developed method (Siano et al., 2018).

2.4. Moisture and ash analysis

The moisture content was determined gravimetrically in triplicate after heating 2.0 g of the TSG sample placed on Pirex glass dishes in an oven at 105 °C for 6 h up to constant weight. For the analysis of ashes, 5.0 g of TSG flour was accurately weighted and incinerated in a muffle furnace at 550 °C until grey ashes and constant weight were obtained. After cooling, ash was weighted, and percent content determined either on dry basis or on wet basis considering moisture.

2.5. Inductively coupled plasma-optical emission spectroscopy (ICP-OES) analysis

About 0.5 g of the TSG sample was weighted in a 250 mL test tube (VELP Scientific, Usmate, MB, Italy) and mineralized with a mixture of HNO$_3$-H$_2$SO$_4$ 12.5:2.5 (v/v) at 180 °C for 3 h until complete destruction of the organic matrix, when samples were transferred into a 25 mL volumetric flask and made up to the mark with double distilled water. The digestion blank was prepared in the same way, without adding the

sample. Elements were determined in triplicate using an Optima 7000 DV ICP-OES (Perkin-Elmer, Waltham, MA, USA) equipped with a Scott-Type Spray Chamber and with a Charge Couplet Detector (CCD), setting axial view and using 1.2 kW RF power, plasma flow rate 15 L min^{-1}, sample flow rate 0.8 mL min^{-1}. Calibration curves were built using a standard 100 mg L^{-1} multielement solution of aluminium (Al), boron (B), calcium (Ca), cadmium (Cd) chromium (Cr), cobalt (Co), copper (Cu), iron (Fe), potassium (K), magnesium (Mg), manganese (Mn), molybdenum (Mo), sodium (Na), nickel (Ni), lead (Pb), phosphorus (P), titanium (Ti), zinc (Zn), silicon (Si) and sulphur (S), which was purchased from CPAchem (Bogomilovo, Bulgaria). Salts of La(NO$_3$)$_3$·6H$_2$O, Ce (SO$_4$)$_2$·4H$_2$O, Nd(NO$_3$)$_3$·6H$_2$O, Gd(NO$_3$)$_3$·6H$_2$O and Dy(NO$_3$)$_3$·4H$_2$O were purchased from Merck KGaA (Darmstadt, Germania). The detection of Gd was confirmed with two additional independent assays, on the same TSG sample performed in technical triplicate in different days.

2.6. Lipid content analysis

Analysis of the fatty acid methyl esters (FAMEs) was performed according to the Association of Official Analytical Chemists, Method 969.33 (AOAC, 1990). FAMEs were obtained through transmethylation carried out on 200 mg of Soxhlet-extracted lipid fraction, which were suspended in 2 mL of 1.25 M HCl/CH$_3$OH solution in Pyrex test tubes with screw caps and incubated in a water bath at 90 °C for 60 min. After the addition of 2 mL of deionized water, FAMEs were extracted with *n*-hexane and filtered using Millex 0.45-μm PVDF disposable syringe filters (EDM Millipore Corp., Billerica, MA, USA).

GC analyses were performed using a 7890A gas chromatograph (Agilent Technologies, Palo Alto, CA, USA) equipped with a flame ionization detector (FID), using a SP-2560, 100 m x 0.20 mm capillary column (Supelco-Sigma-Aldrich). FAME extracts (1 μL) were introduced through a split-splitless injection system of an AS 3000 autosampler in split mode (ratio 1:100) at 260 °C. The oven temperature program started at 140 °C (held for 5 min) and linearly increased to 260 °C (4 °C min^{-1}) up to the end of the analysis. FID temperature was 260 °C. FA composition of TSG was obtained by comparison with the retention time of the standard mixture FAME 37 components (Sigma) and was expressed as percentage area.

For the analysis of phytosterols, Soxhlet-extracted lipids (200 mg) were saponified in 2 mL of 2 M KOH in 80 % (v/v) aqueous ethanol. The unsaponifiable fraction was twice extracted in 2 mL diethyl ether and washed with water until neutral reaction. Ether phase was dehydrated with anhydrous sodium sulfate, filtered on paper, and dried under vacuum. The residue (100 μL) was dissolved in 50 mL of hexane and 1 μL was analysed by GC-FID using the same chromatograph as above, equipped with an RTX-5 30 m × 0.25 mm × 0.25 μm column (Restek, Bellefonte, PA, USA). Samples were introduced through the autosampler in 1:10 split mode at 250 °C. The oven temperature program started at 200 °C (held for 2 min) and linearly increased to 300 °C (20 °C min^{-1}) to the end of the analysis. FID temperature was 260 °C. A plant sterol mix (Matreya, State College, PA, USA) was used as the external standard for compound identification. Relative abundance was obtained by software assisted peak integration (Chemstation vers. B04.03, Agilent) and was expressed as percentage area.

2.7. Protein content analysis

Total crude protein of germ flour samples was determined through the Kjeldahl method using an automated analyzer (BÜCHI K350, Switzerland) using 6.25 as the nitrogen conversion factor (AOAC, 2001).

2.8. Preparation of germ proteins for electrophoresis analysis

TSG flour samples (100 mg) were defatted with five volumes (*w/v*) of diethyl ether under magnetic stirring for 10 min (twice). Proteins were extracted by 1 mL of a denaturing (7 M urea, 50 mM Tris-HCl pH 8.0,

150 mM NaCl) or denaturing/reducing (including 10 mM dithiothreitol, DTT), buffer for 1 h under magnetic stirring at room temperature. Flour was then centrifuged at 10,000 *g* for 30 min and the supernatant collected. Finally, proteins were desalted against 25 mM ammonium bicarbonate (AMBIC) using Econo-Pac DG column (Bio-Rad, Milan, Italy), quantified using the Bradford assay (Bio-Rad), lyophilized and stored a −26 °C.

2.9. SDS-PAGE analysis

For the mono-dimensional SDS-PAGE (Bio-Rad, Mini-Protean) on precast linear gels (TGX Gel 12 % acrylamide), protein extracts were dissolved in Laemmli buffer (0.125 M Tris-HCl pH 6.8, 5 % SDS, 20 % glycerol, 5 % (w/v) β-mercaptoethanol, 0.02 % bromophenol blue) at a 2.0 μg μL^{-1} concentration and denatured in a boiling water bath for 5 min. A final volume of 10 μL was loaded onto the SDS-PAGE wells. Analysis under nonreducing conditions was carried out in the same way of reducing SDS-PAGE but omitting β-mercaptoethanol. Electrophoresis was performed at constant voltage (100 V) at room temperature. After migration, the gels were stained with Coomassie Blue R-250 and imaged with a LABScan scanner (GE Healthcare, Uppsala, Sweden). For - proteomic analysis, protein bands were manually excised, destained with acetonitrile/25 mM AMBIC (1/1, v/v) and dried under vacuum after dehydration in acetonitrile. Gel pieces were rehydrated with 20 μL of a 12 μg μL^{-1} proteomic grade modified trypsin (Pierce/Thermo, Rockford, IL, USA) solution in 50 mM AMBIC for 45 min on an ice-cold bath. Afterward, the excess of trypsin solution was discarded, and the protein bands were incubated overnight at 37 °C. The tryptic peptides were two-fold extracted in 40 μL of 50 % acetonitrile containing 2.5 % (v/v) formic acid and dried using a speed-vac.

2.10. Shotgun proteomics

To prepare protein samples for shotgun proteomics, an aliquot of the TSG protein, extracted in denaturing/reducing (10 mM DTT) conditions and Cys-alkylated with 55 mM iodoacetamide as described, was desalted against 25 mM AMBIC, pH 7.8, using the Econo-Pac 10 DG (Bio-rad) size exclusion columns. Proteins were quantified with the Bradford assay and incubated overnight at 37 °C with proteomic grade trypsin at an enzyme-to-substrate ratio 1/50 (w/w). Resulting peptides were purified on reverse phase C18 spin columns (Pierce/Thermo), by washing with 0.1 % (v/v) trifluoroacetic acid (TFA) and eluting with 65 % acetonitrile/0.1 % TFA. Purified peptides were finally vacuum dried and reconstituted with 0.1 % formic acid.

2.11. Nanoflow-HPLC-ESI-MS/MS analysis

Mass spectrometry analysis of in gel digested bands was performed using a Q Exactive Orbitrap mass spectrometer (Thermo Scientific, San Jose, CA, USA), online coupled with an Ultimate 3000 ultra-high performance liquid chromatography instrument (Thermo Scientific). Samples were resuspended in 0.1 % (v/v) formic acid solution, loaded through a 5 mm long, 300 μm i.d. pre-column (LC Packings, USA) and separated by an EASY-Spray™ PepMap C18 column (2 μm, 15 cm × 75 μm) 3 μm particles, 100 Å pore size (Thermo Scientific). Eluent A was 0.1 % formic acid (v/v) in Milli-Q water; eluent B was 0.1 % formic acid (v/v) in acetonitrile. The column was equilibrated at 5 % B. Peptides were separated applying a 4–50 % gradient of B over 60 min at a flow rate of 300 nL min^{-1}. The mass spectrometer operated in data-dependent (top 5 ions) mode acquiring MS full scan spectra acquired in the 300–1600 m/*z* range in the positive ionization mode with a resolving power of 70,000 and 17,500 full width at half maximum (FWHM) for MS and MS/MS fragmentation spectra, respectively. A dynamic exclusion of 10 s was applied for the MS/MS selection. For the shotgun proteomic analysis, samples were analyzed in triplicate with the same conditions above, injecting 2 μg peptides for each run.

LC-MS/MS runs were elaborated using the Xcalibur Software 3.1 version (Thermo Scientific) and converted in mgf file using the MsConvert (https://proteowizard.sourceforge.io/index.html) application for protein identification. The mgf files were used to interrogate SwissProt (updated June 2021) and the UniprotKB (updated September 2020) databases using the open-source Mascot MS/MS ion search (https://www.matrixscience.com/) and the Batch Tag Web (https://prospector.ucsf.edu/prospector/mshome.htm) search engines, respectively.

Database searching parameters were the following: Met oxidation and pyroglutamic for N-terminus Gln as variable protein modifications; Cys-carbamidomethylation as a constant modification; a mass tolerance value of 10 ppm for precursor ion and 0.01 Da for MS/MS fragments; trypsin as the proteolytic enzyme with up to 2 missed cleavage. Searches were taxonomically restricted to Green Plants. Due to the lack of protein entries for *Caesalpinia spinosa*, proteins were identified by homology and the band identifications were accepted when proteins were identified with at least 3 peptides at a false discovery rate of 0.01 (target decoy validation).

Gene Ontology (GO) enrichment and functional classification analyses were carried out with the list of filtered proteins identified with at least two unique peptides, using the open source ShinyGO v0.75 with the automatic best matching species option (https://bioinformatics.sdstate.edu/go/).

2.12. Polyphenol extraction

TSG samples (100 mg in triplicate) were sequentially extracted with 1 mL methanol, 1 mL 80 % aqueous methanol (v/v) and 1 mL 80 % aqueous ethanol (v/v). The slurry was centrifuged at 10,000 $g \times$ 15 min at room temperature between consecutive extraction steps and the supernatants were combined. The yellow-colored extracts were filtered using 0.22 μm PVDF disposable syringe filters (Millex, Millipore, Badford, MA, USA) and stored at − 26 °C until analysis.

2.13. Total polyphenols, radical scavenging activity and antioxidant capacity

The concentration of total phenols (TPC) in the extracts was determined by the Folin-Ciocalteu colorimetric method, using the general procedures recommended by the European Pharmacopoeia for the determination of total tannins (European Pharmacopoeia, 2007), monitoring the absorbance at 760 nm with a UV–Vis spectrophotometer (Amersham Ultrospec 2100 Pro UV/Vis, GE Healthcare, Uppsala, Sweden). Gallic acid within the 50–500 mg L^{-1} concentration range was used as the standard. TPC was expressed as g kg^{-1} of gallic acid equivalents (GAE). Samples were assayed in triplicate. Radical scavenging activity of the polyphenol extracts from TSG and, in comparison, from carob seed germ flour was assessed with the DPPH assay against a calibration curve built with 50–500 mg L^{-1} gallic acid. Values are expressed as g$_{GAE}$ kg^{-1}. DPPH inhibition of 1 % (w/w) aqueous methanolic (80 %, v/v) solutions of TSG and carob seed germ flour was determined as previously detailed (Siano et al., 2023a), while the antioxidant capacity was determined as CDAC (coulometrically determined antioxidant capacity) according to a recently developed coulometric method (Siano et al., 2023b).

2.14. RP-HPLC

TSG hydroalcoholic extracts were separated using a modular HP 1100 chromatographer (Agilent Technologies, Paolo Alto, CA, USA) equipped with a diode array detector (DAD). The stationary phase was a 250 × 2.0 mm i.d. C18 reversed-phase Jupiter column, 4 μm particle diameter (Phenomenex, Torrance, CA, USA). The column temperature was maintained at 37 °C during the HPLC analyses. Runs were performed at a constant flow rate of 0.2 mL min^{-1} applying a 5–60 % linear gradient of the solvent B (acetonitrile/0.1 % TFA) after 5 min of isocratic

elution at 5 % B. Solvent A was 0.1 % TFA in HPLC-grade water. For each analysis, 10 μL of combined extracts 10-fold diluted with 0.1 % TFA were injected. Samples were run in triplicate, at least. DAD was set-up to acquire an UV–Vis spectrum every second between 200 and 600 nm. The HPLC separations were monitored at 520, 360, 320 and 280 nm.

For the HPLC analysis of tara proteins, the extracts in reducing and non-reducing conditions (1 mL) were desalted with Econo-pac DG (Bio-Rad) against 25 mM AMBIC and separated on a C4 reversed phase Jupiter® column (250 mm, 2.1 mm i.d., 5 μm particle diameter, 300 Å, Phenomenex), applying a 25–50 % B linear gradient over 40 min (eluents A and B as above). The eluate was monitored at 214 and 280 nm. Chromatograms were elaborated with the ChemStation software vers. A.07.01 (Agilent Technologies).

2.15. Statistical analysis

All parameters were determined at least in triplicate and results were expressed as means ± SD. The calibration curves, graphs and figures were generated using the OriginPro 2016 software (OriginLab, Inc., Northampton, MA, USA).

3. Results and discussion

3.1. Proximate composition of tara seed germ

The proximate composition of TSG flour is summarized in Table 1. In close agreement with previous data (Re-Jiménez & Amadò, 1989; Borzelleca et al., 1993), proteins were 41.6 and 43.4 %(w/w) of the wet and dry flour, as determined with the Kjeldahl method using 6.25 as the nitrogen conversion factor. The protein content is expected to vary within a limited range depending on the variable presence of residual endosperm and, presumably, on plant related biotic and abiotic factors. Based on a previous report, TSG proteins have a nutritionally interesting amino acid distribution, typical of legume seed proteins, especially regarding essential amino acid content. In particular, TSG flour exhibited better amino acids distribution and higher nutritional quality compared to related carob and guar germ flours (Re-Jiménez & Amadò, 1989). Total lipids (13.5 and 14.0 %, w/w, on a wet and wry basis, respectively), which were determined by gravimetry after Soxhlet extraction in diethyl ether, and ash content (6.3 and 6.5 % of the wet and dry flour, respectively) were in strict agreement with previously reported values for TSG (Re-Jiménez & Amadò, 1989) and both appeared particularly high. The proximate composition of TSG was also assayed using ATR-FTIR by comparison with a carob seed germ flour having a protein content of 44.3 and 48.9 % (w/w) on a wet and dry basis, respectively (Fig. 1). In both cases, the shape of the broad band centred at 3279 cm^{-1} proved the prevalence of the N–H stretching over the O–H stretching as a result of the high protein content. The amide I and amide II bands at 1639 and 1537 cm^{-1}, respectively, were somewhat less intense for TSG than for the carob counterpart, consistent with the slightly less abundant protein content. In contrast, the carbonyl stretching band at 1745 cm^{-1} was more intense for TSG confirming the higher abundance of lipids compared to the carob seed germ flour. The relatively intense vinyl stretching at 3010 cm^{-1} testifies the abundance of TSG unsaturated fatty acids within the lipid fraction (see below). The

Table 1
Proximate composition of tara germ flour.

Component crude content	g 100 g^{-1} (FW)	g 100 g^{-1} (DW)
Moisture	4.2 ± 0.1	–
Protein	41.6 ± 0.8	43.4 ± 0.8
Carbohydrates[a]	34.4 ± 0.6	35.8 ± 0.5
Lipid	13.5 ± 0.4	14.0 ± 0.5
Ash	6.3 ± 0.2	6.5 ± 0.3

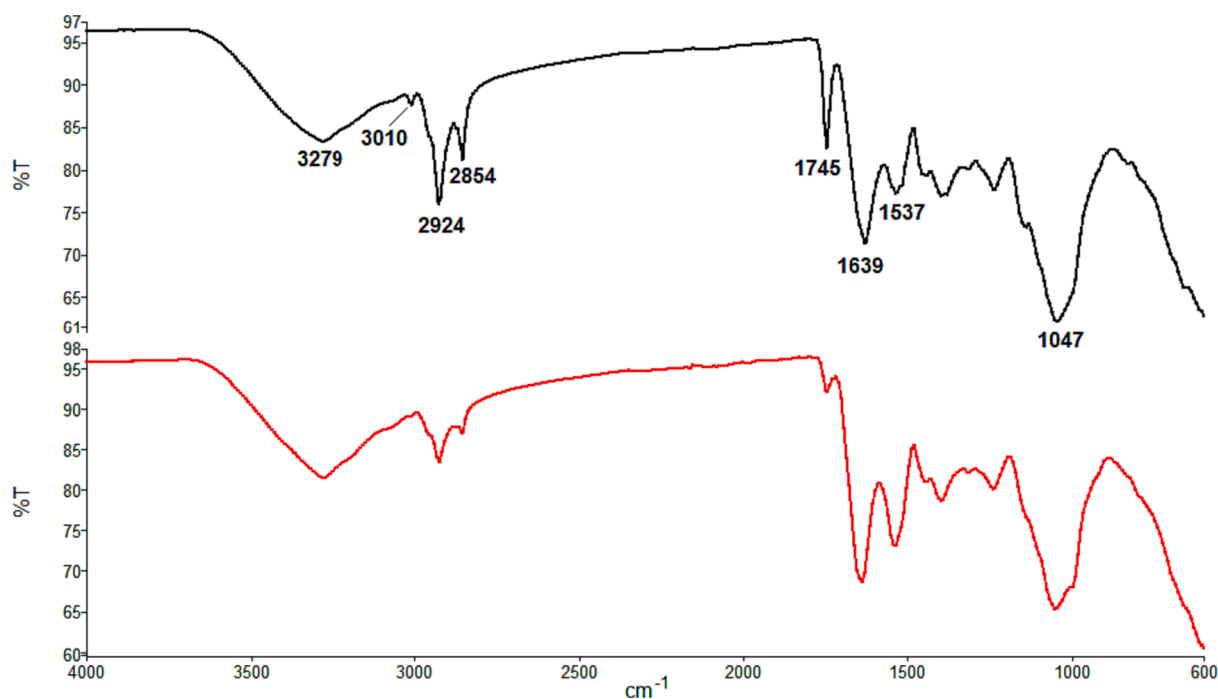[a] Carbohydrate content was determined by the difference method.

Fig. 1. ATR-FTIR comparison between tara (black line) and carob (red line) germ flours. (For interpretation of the references to color in this figure legend, the reader is referred to the web version of this article.)

broad band centred at 1047 cm^{-1} corresponding to the fingerprinting region of carbohydrates was practically overlapping between the two flour samples.

3.2. Ash and element composition

Ash constitutes the residual inorganic fraction of food after combustion at high temperatures. Although the ash content varies within a relatively limited range in conventional food flours (0.1–2.5 %, w/w), the mineral elements contained therein play main functional and micronutrional roles (Bilge et al., 2016). The ash content of TSG flour was found strikingly high, accounting for 6.3 and 6.5 % of the wet and dry weight, respectively, indicating that tara plants tend to uptake soil minerals and accumulate them in the germ. Notably, *Ceasalpinia* spp. and related plants are strong absorbers of metals, so that their leaves have been proposed as bioindicators of soil pollution (Rolli, Karalatti, & Gadi, 2015). For this reason, in some Andean regions tara trees are cultivated for phytoremediation purposes. In view of the relatively high ash content, the element composition was determined using ICP-OES (Table 2). Analytical data demonstrates that TSG flour is particularly rich in P, K, Ca, and Mg, whereas the relative Na content is considerably lower. Other elements, such as Fe, Zn, Mn, and Cu, occur at nutritionally interesting levels. The presence of Gd (gadolinium) at a concentration of 1.6 mg kg^{-1} and traces of Dy (dysprosium) perhaps reflects the Andean origin of the plant, even though its accumulation in seeds and plants could be a consequence of anthropogenic pollution as well (Zhang et al., 2019). Generally, lanthanides naturally occur as extremely insoluble phosphate salts. The detection of only Gd and traces of Dy among lanthanides could reflect the relatively lower insoluble character of their salts (Firsching & Brune, 1991) or the TSG origin which might be cultivated on accidentally contaminated soils. Free Gd ions are highly toxic to several target human organs, liver and brain included, while the toxicity of chelated Gd decreases by more than 30 times as in the case of its controlled use as a contrast medium in diagnostic tests (Davies, Siebenhandl-Wolff, Tranquart, Jones, & Evans, 2022). Gd ions can compete with calcium ions and penetrate in the hepatocytes, blocking calcium-dependent protein channels. Gd inhibits hepatic microsomal

Table 2
Mineral composition of tara germ flour analyzed. * below the limit of detection (0.1 mg kg^{-1})

Element	Concentration Unit	Fresh weight (FW)
P	g kg^{-1}	19.4 ± 0.6
K	g kg^{-1}	15.9 ± 0.7
Ca	g kg^{-1}	9.5 ± 0.3
Mg	g kg^{-1}	4.8 ± 0.2
Na	mg kg^{-1}	65.2 ± 1.3
Zn	mg kg^{-1}	62.2 ± 1.0
Fe	mg kg^{-1}	36.9 ± 0.8
B	mg kg^{-1}	35.1 ± 0.5
Al	mg kg^{-1}	23.5 ± 0.7
Mn	mg kg^{-1}	23.4 ± 0.4
Cu	mg kg^{-1}	17.3 ± 0.8
Mo	mg kg^{-1}	1.6 ± 0.2
Co	mg kg^{-1}	1.3 ± 0.2
Cr	mg kg^{-1}	– *
Ti	mg kg^{-1}	– *
Pb	mg kg^{-1}	– *
Cd	mg kg^{-1}	– *
Ni	mg kg^{-1}	0.8 ± 0.1
Ce	mg kg^{-1}	– *
Nd	mg kg^{-1}	– *
Gd	mg kg^{-1}	1.6 ± 0.1
La	mg kg^{-1}	– *
Dy	mg kg^{-1}	trace

epoxide hydrolase and glutathione S-transferases and affects the dose-inhibitory response curves for protein kinase C inhibitors, which are suppressors of drug metabolizing enzymes (Pałasz & Czekaj, 2000).

Thus, Gd or other lanthanides might be responsible for the acute toxicity effects triggered by some TSG batches. Currently, the safety threshold for human exposure to Gd is not known, but it might be very low. In the investigated sample, the Gd level is likely insignificant, also considering that TSG is used as a minority ingredient in food preparations. Indeed, no adverse effects have been associated with the consumption of the large TSG batch from which the assayed sample has been obtained. However, our results suggest that metal ions could

accumulate in tara seed embryo and TSG could be contaminated to varying degree and with different metal ions depending on the specific plant growing area. This hypothesis would explain why known reports of adverse effects appear limited to a single or a few production batches.

It must be emphasized that the Gd- or other lanthanides-induced toxicity of TSG is only a speculative hypothesis, which has been formulated without having available clinical data of injured individuals. This assumption requires confirmation through dedicated toxicological studies over a statistically significant number of flour samples. If the hypothesis of accidental contamination is confirmed, TSG could be allowed for human or animal consumption provided that the presence of the harmful agent in the flour is prevented and monitored.

3.3. Lipids

Total lipids of TSG are significantly higher than in the carob and *Prosopis* spp. counterparts (7–8 %, w/w, of which 9.5–11.8 % phospholipids) (Siano et al., 2018), while the relative content of phospholipids is lower, accounting for 5.1 % (w/w) of the lipid fraction, as estimated using a previously detailed ATR-FTIR-based method (Siano et al., 2018). In opportune proportions, polar lipids such as lecithin improve the fermentation behaviour of yeast dough, loaf volume, and crumb structure, contribute to delay bread staling, and stabilize emulsion in creams, foams, and mousses. By virtue of the significant content of polar lipids in absolute terms, TSG flour could be an interesting ingredient for technological applications either as a pure flour or as a fortifier of other baking flours or as an emulsifier in creams, mousses, and protein beverages. The distribution of fatty acids was determined by GC-FID after transmethylation and is summarized in Table 3. The largely predominant fatty acid is linoleic acid ($C_{18:2}$, ω-6), which constitutes 2/3 of the total fatty acids. The relative content of linoleic acid in triacylglycerols (TAG) is higher than that of carob and *Prosopis* spp. germ, while oleic acid ($C_{18:1}$, ω-9) of TSG is 10.9 %, which is about half that of the latter species. In agreement with a previous report, asclepic or *cis*-vaccenic acid ($C_{18:1}$, ω-7*c*) occurs at 4.85 % (Rahanitriniaina, Artaud, Iatrides, & Gaydou, 1984). TSG is particularly rich in polyunsaturated fatty acids (PUFA) and can contribute to supply essential linoleic acid. On the other hand, PUFA can render tara germ susceptible of autoxidation, thus in principle affecting stability of flour and shelf life of the derived products. Similar to the germ of *Prosopis* spp., TSG contains almost 2.5 % of very long chain fatty acids, such as behenic ($C_{22:0}$) and

lignoceric ($C_{24:0}$) acids (Rahanitriniaina et al., 1984), which may exert health-promoting effects in humans (Abedi & Sahari, 2014). Although very long chain fatty acids are rather rare in most of the foods ordinarily consumed, they are extensively investigated for several reasons, including: i) biosynthetic activity in developing seeds; ii) capability to confer the entire lipid fraction with plastic properties; iii) potential role as dietary precursors of lipid signalling mediators involved in a number of human physio-pathological pathways (Lee, Cho, & Shin, 2015). Interestingly, the GC-FID analysis excluded the presence of potentially harmful fatty acids at detectable amount, such as erucic or ricinoleic acids.

The unsaponifiable fraction constitutes around 2.5 % (w/w) of the TSG lipid fraction. β-sitosterol is the most represented phytosterol (64.10 % of the sterol fraction) and stigmasterol ranks as the second (9.67 %), while brassicasterol was not detected. Squalene and tocopherols are not particularly high, and their content is comparable to those of carob and *Prosopis* spp. seed germ (Siano et al., 2018).

The GC-FID chromatograms of TSG fatty acids (as fatty acid methyl esters) and phytosterols are shown in **Supplementary information Figure S1**.

3.4. Preliminary proteomic characterization of TSG

The SDS-PAGE separations of TSG proteins under reducing (+β-ME) or nonreducing (- β-ME) conditions are compared in Fig. 2. The electrophoretic protein patterns resemble those previously found in carob (*Ceratonia siliqua*) seed germ flour (Mamone et al., 2019). Labelled protein bands were excised, destained, Cys alkylated, in gel digested with trypsin, and the resulting tryptic peptides were analyzed by LC-MS/MS. Practically, there is no protein annotation in the UniprotKB database for *Caesalpinia spinosa* and taxonomically related species. For this reason, protein bands were assigned by homology with sequenced storage proteins of plant seeds. An accurate homology analysis was carried out with the Mascot search engine in the Swiss-Prot database and then further enlarged with the Batch-Tag Web tool of Protein-Prospector in the UniprotKB database. The proteins identified by interrogating the Swiss-Prot and the UniprotKB databases are inventoried in Supplementary **Table S1** and Supplementary Tables S2-S14, respectively. The partial discrepancy in the lists of proteins identified with the two approaches was expected and depends on the difference in the two databases queried and on the different search algorithms. Anyway, like most dicotyledonous plant seeds, 11S globulin-like subunits, which were assigned by homology with the 11S globulin subunits of pumpkin (*Cucurbita maxima*) or sunflower (*Helianthus annus*) seeds, appear as the largely dominant storage proteins of TSG. The 11S subunits were detected in many electrophoretic bands covering a very large molecular weight range, likely due to either aggregation or proteolytic events. Nevertheless, the 11S globulin-like subunits were particularly abundant in relatively intense bands n. 4, 5, 6 and 7, as assessed by the number of unique matching peptides. In general, 11S globulins are composed of varying subunits. For example, at least six and five different major subunits of 11S globulin have been identified in sunflower seed embryos and soybean (*Glycine max*), respectively (Adachi et al., 2003; Quiroga et al., 2013). The 11S proglobulin subunits are post-translationally cleaved at an evolutionarily conserved Asn-Gly bond into mature acidic and basic domains, which are still bound together by a disulphide bridge. In reducing conditions, the acidic and basic domains are split apart in the SDS-PAGE and migrate approximately at ca. 36 kDa (bands n. 4 and 5) and, at ca. 26 kDa (band n. 7) and ca. 24 kDa (bands n. 8 and 9), respectively. The relative abundance of 11S globulin-like protein in several distantly or closely migrating bands and the distribution of acidic and basic subunits probably results from the occurrence of multiple proteoforms that undergo a typical chain trimming at the protein terminal ends (Nitride, Picariello, Mamone, & Ferranti, 2017). In nonreducing conditions, only a small fraction of the 11S globulin migrated at apparent molecular weight corresponding to the
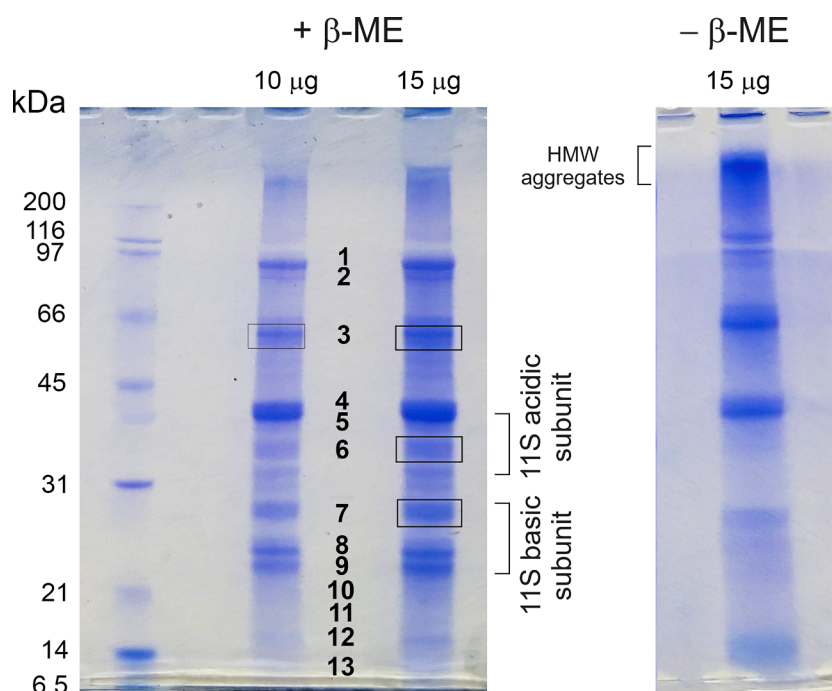
Table 3

Lipid fraction of tara germ flour: Fatty acid (as FAME) and phytosterol composition. * below the limit of detection (0.01%)

Fatty acids	(% area)
Palmitic, C16:0	9.85 ± 0.43
Palmitoleic, C16:1	0.44 ± 0.02
Stearic, C18:0	3.27 ± 0.12
Oleic, C18:1, ω-9*c*	10.86 ± 0.36
Asclepic (*cis*-vaccenic), C18:1, ω-7*c*	4.85 ± 0.15
Linoleic, C18:2, ω-6*c*	66.07 ± 0.83
Arachidic, C20:0	0.82 ± 0.03
Linolenic, C18:3, ω-3	1.21 ± 0.04
cis-11-Eicosenoic, C20:1	0.15 ± 0.02
Behenic, C22:0	2.20 ± 0.07
Lignoceric, C24:0	0.28 ± 0.05
Σ-SFA	16.42 ± 0.46
Σ-MUFA	16.29 ± 0.39
Σ-PUFA	67.29 ± 0.83
Σ-PUFA/Σ-SFA	4.09 ± 0.20
Unsaponifiable fraction (2.5 % w/w of lipids)	(% area)
Squalene	2.59 ± 0.09
Brassicasterol	_ *
Campesterol	4.24 ± 0.18
Stigmasterol	9.67 ± 0.35
β-sitosterol	64.10 ± 1.12
Δ5-avenasterol	2.54 ± 0.08

Fig. 2. SDS-PAGE analysis of tara seed germ protein analyzed in reducing (+β-ME) and non-reducing (- β-ME) conditions. Numeric labels indicate the protein bands excised for proteomics analysis. Main proteins in individual bands are assigned in Supplementary information Tables.

combination of acidic and basic subunits (ca. 62 kDa). Indeed, the nonreducing SDS-PAGE analysis featured the presence of very high molecular weight protein aggregates (Fig. 2, **right panel**), mainly due to supramolecular aggregation of the 11S globulin subunits, alongside the monomeric form (ca. 62 kDa) and low abundance acidic (ca. 36 kDa) and basic subunits (ca. 26 and 24 kDa) of this protein already split, as assessed by LC-MS/MS analysis of the tryptic digest. The detection of very large protein aggregates matches with the formation of sticky macroparticles visible during the post-extraction storage of the protein solutions. The HPLC analysis of TSG protein extracts before and after reduction confirmed the split of the acidic and basic subunits of 11S globulin as shown in Fig. 3, in which protein peaks were putatively assigned based on the hydrophobicity of the polypeptide chains.

An ATP-dependent Clp protease (ca. 84 kDa) related to the heat shock protein 70, which was identified by homology with *Lupinus albus* and *Triticum urartu*, and a luminal binding protein (ca. 71 kDa) that promotes the assembly of multimeric protein complexes were the most represented gene products in the electrophoretic bands n. 1 and 2, respectively. Peptides of a 7S-like vicilin, identified by homology with hazelnut (*Corylus avellana*) were also detected in bands n. 2 and n. 4. Both 11S (legumin) and 7S (vicilin) storage proteins belong to the cupin superfamily and are major plant food allergens (Mills et al., 2002). However, clinical evidence excluded that the adverse effects caused by TSG could be correlated with allergic reactions (Chittiboyina et al., 2023).

Several metabolic and ribosomal proteins (*e.g.*, 50S and 30S ribosomal protein subunits) were identified in different bands, consistent with the physiological role of the germ, and it should be not surprising that multiple gene products were detected even in well-resolved individual electrophoretic bands, considered the high sensitivity and resolution of the mass spectrometry-based analysis.

To broaden the protein characterization of TSG, a gel-free shotgun proteomic analysis was carried out. Protein identifications were filtered (Supplementary Table S15), saving only the best matching protein entries, or reported as unfiltered, maintaining the interesting homologous protein matches, to catalogue typology and function of uncharacterized gene products (Supplementary Table S16). With the shotgun proteomic
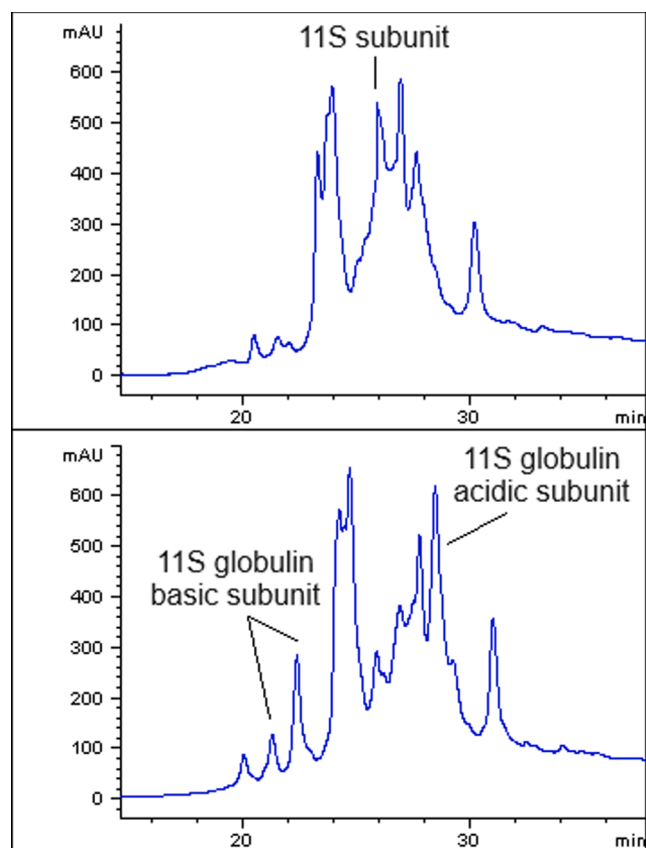

Fig. 3. RP-HPLC analysis (λ = 214 nm) of tara germ protein extracts in non-reducing (upper panel) or reducing conditions (lower panel).

analysis, the 11S globulin was detected but it appeared no longer as the top-ranking protein. In contrast, top protein entries included elongation factors, heat shock proteins, metabolic enzymes, especially those

involved in protein biosynthesis. However, since proteins were assigned by homology and matching peptides depend on the degree of conserved sequences, it is not possible to infer protein abundance. Several proteins involved in the abiotic stress of the plant were inventoried, such as the late embryogenesis abundant proteins. Many peptide MS/MS spectra remained unassigned, due to the lack of specific sequences in the genomic and proteomic databases. A gene ontology (GO) functional enrichment analysis of the gene products identified in TSG was carried out with the open-source bioinformatic tool ShinyGO v0.75 with automatic selection of the best matching species. The gene products identified by homology and catalogued by the software were classified according to the Biological Process and Molecular Function (Fig. 4). Although only a part of the 358 filtered gene products (Supplementary Table S15) were functionally classified, it appears clear that most of the TSG proteins are metabolic enzymes involved in both catabolic breakdown of seed storage biomolecules and biosynthesis of new functionally active enzymes, to obtain energy and chemical building-blocks required by the germination process.

Hemagglutinating proteins were not detected by either in-gel or gel-free proteomics, in keeping with the biological assays (Chittiboyina et al., 2023). Similarly, homologues of α-amylase and protease inhibitors, related to legume sourced Kunitz-type of Bowman-Birk inhibitors, were not identified although previously suggested (Grobbelaar, Pollard, & Steward, 1955). The presence of these anti-nutritional factors cannot be ruled out due to the incompleteness of the proteomic characterization. The occurrence of protease inhibitors in TSG and the
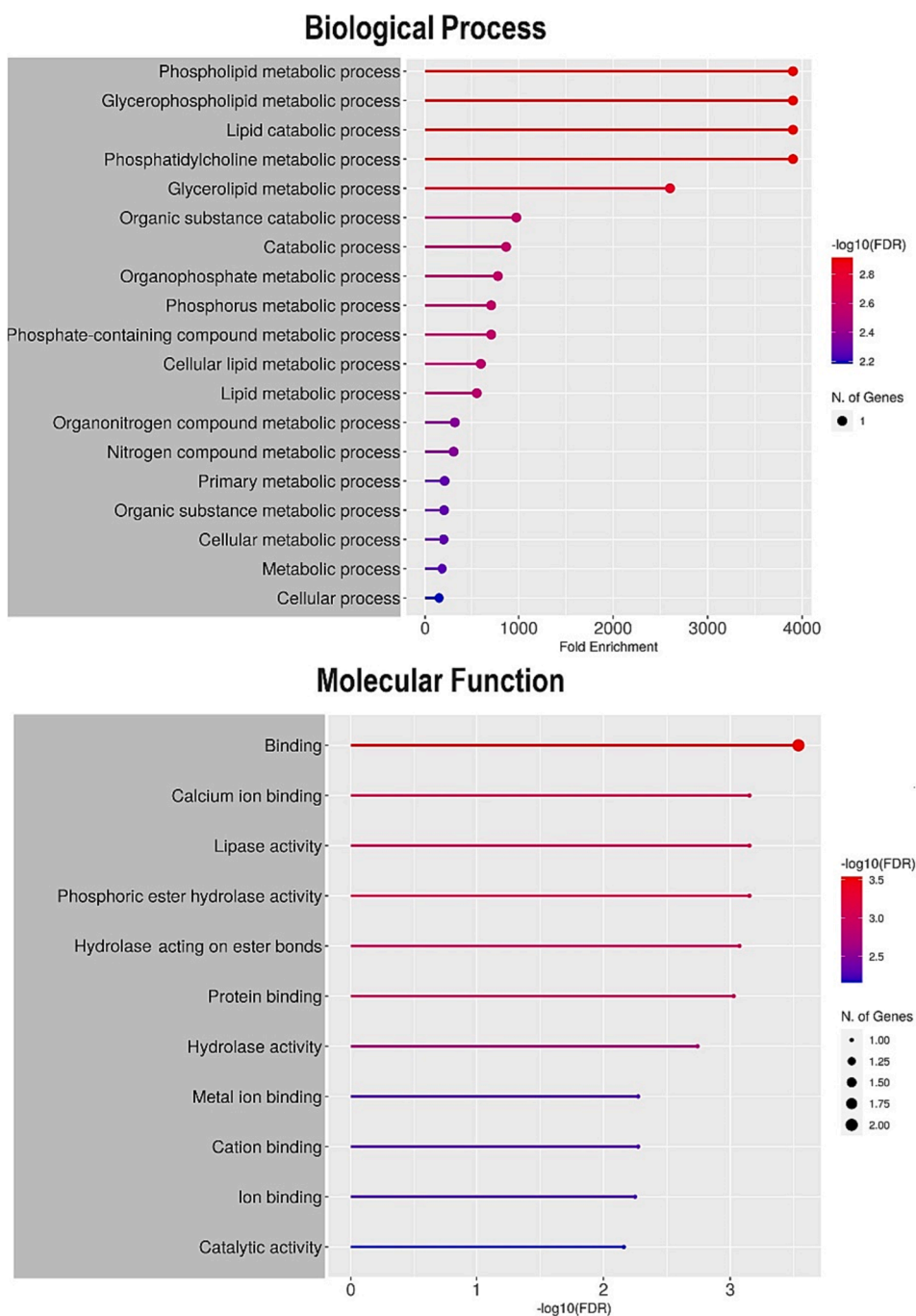

Fig. 4. GO functional classification of TSG proteins according to the Biological Process and the Molecular Function. The functional and enrichment analyses were carried out using the list of filtered proteins identified with at least two unique peptides (Supplementary Table S15).

possibility of deactivating them by thermal treatments is an interesting aspect to be investigated. Anyway, it appears unlikely that protease inhibitors can elicit acute toxic effects (Lajolo & Genovese, 2002).

3.5. Polyphenols

TSG flour is intensely yellow-coloured, with more pronounced shades than the carob counterpart. The yellow pigments of TSG flour are soluble in 80 % (v/v) methanol, suggesting a high content of flavonoids. Total polyphenols, determined with the Folin-Ciocalteu method, were 14.9 g_{GAE} kg^{-1}, which abundantly exceeds the figures for carob and *Prosopis* spp. germ (Picariello et al., 2017). The DPPH radical scavenging activity of TSG was 16.8 g_{GAE} kg^{-1} which is more than double than the one determined for the carob germ flour (7.6 g_{GAE} kg^{-1}). Similarly, the DPPH radical inhibition of a 1 % (w/w) solution of TSG was 43.1 %, much higher than for the carob counterpart (23.9 %). Antioxidant capacity of the two extracts was assayed with a recently developed coulometric method (Siano et al., 2023b). CDAC of TSG was 624 mmol e^{-} kg^{-1}, which is a value comparable to many common pure antioxidants (Siano et al., 2023b) and was 3.5 times higher than the carob counterpart (178 mmol e^{-} kg^{-1}). Overall, these figures highlight the excellent antioxidant capacity of TSG, which could promote several benefits on human health. HPLC-DAD separation of TSG polyphenol extracts evidenced intense peaks of gallic acid (retention time = 7.7 min, λ_{max} = 268 nm) and several flavonoids most likely attributable to glycosides of apigenin, as assessed by the typical UV–Vis spectrum with a $\lambda_{max} \approx 334$ nm. On the other hand, only a few minor peaks of the TSG extract correspond to the dominant apigenin *C*-glycosides of the carob germ, which have been identified as schaftoside (*i.e.*, apigenin 6-*C*-glucoside-8-*C*-arabinoside) and isoschaftoside (*i.e.*, apigenin 6-*C*-arabinoside-8-*C*-glucoside) (Fig. 5). The most intense peak of TSG polyphenols likely is vicenin-2, that is apigenin 6,8-di-*C*-glucoside (Chittiboyina et al., 2023), while the structure of the other congeners remains to be elucidated. Given the structural correlation of the phenolic substances of TSG with those of carob and Prosopis *spp*. germ, for which no cases of toxicity have

been reported so far, and the presence of apigenin *C*-glycoside derivatives in many common food matrices (Bucar et al., 2021), it is unlikely that one or some components of this class could be responsible for toxic effects. The interest in structure and potential health-promoting effects of TSG flavonoids guarantees their systematic characterization in a forthcoming dedicate study.

4. Conclusion

TSG is a sustainable source of plant proteins and has the potential to be used as a food ingredient with excellent functional and nutritional properties. The demand for hydrocolloids such as those deriving from carob, tara and guar seeds by cosmetic, food and pharmaceutical industries is sharply growing. Therefore, most likely TSG will become widely available in the near future. To the best of our knowledge, there is no documented data on the volume of TSG used yearly for human and animal consumption. It is certain, however, that it has been used extensively for these purposes, also as a source of protein hydrolysates, alongside homologous carob, and guar germ flours (Re-Jiménez & Amadò, 1989). Therefore, from a regulatory point of view conflicting opinions have been formulated on whether to consider TSG as a source of novel proteins. Although many producers of tara gum are still advertising TSG as a food or feed ingredient on their websites, safety concerns have rightly warned about its use until the origin of the adverse events is ascertained. In the last few months, extensive testing has excluded many possible hazards, including xenobiotics, food allergens, microbial and chemical contaminants. One of the most accredited hypotheses, although not definitive, is that the cause of the recorded adverse events are *in vivo* produced metabolites of nonprotein amino acids, especially baikiain, that inhibit liver enzymatic targets (Chittiboyina et al., 2023). The data of the current study provide previously unavailable information about TSG. This study reliably rules out the presence of anti-nutritional protein factors, allergens, fatty acids, and harmful phenolic substances, and suggests, through exclusion criteria, that an accidental contamination with rare earth elements, such as
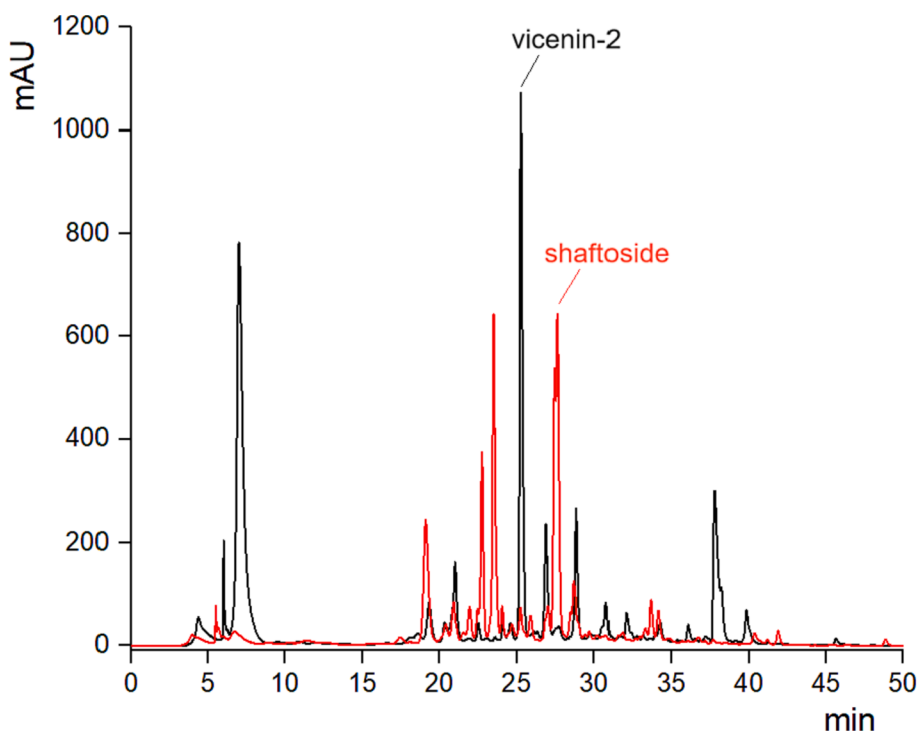

Fig. 5. RP-HPLC comparison of 80% (v/v) methanol extracts from tara (black line) and carob (red line) germ flour. The most abundant polyphenol compounds of tara and carob germ flours are vicenin-2 and schaftoside, respectively. Gallic acid is particularly high in tara germ flour. (For interpretation of the references to color in this figure legend, the reader is referred to the web version of this article.)

gadolinium, might be a different working hypothesis for establishing the cause of adverse events. One of the limitations of this investigation is certainly the fact that only one sample of TSG was characterized. However, the availability of TSG is very limited since the extraction processes of tare gum are carried out only in a few regions of the world and many food companies have now discontinued supplying flour. Considering that TSG is an agro-industrial by-product with excellent properties, which could support the economy of producers and growers of marginalized areas, there remains an urgent need of systematic investigations to definitively establish the causative agent of the reported TSG-induced adverse events and to assess the risk associated with TSG consumption. This work represents a starting point for a necessary collaborative effort to understand whether the harmful agent is a constitutive component of TSG, which would therefore preclude its human and probably also animal consumption unless detoxifying treatments, or a random avoidable contamination, which concerns only some production batches.

CRediT authorship contribution statement

Olga Fierro: Writing – original draft, Methodology, Investigation, Formal analysis, Conceptualization. **Francesco Siano:** Writing – original draft, Methodology, Investigation, Formal analysis, Conceptualization. **Mariacristina Bianco:** Formal analysis. **Ermanno Vasca:** Writing – original draft, Methodology, Investigation, Conceptualization. **Gianluca Picariello:** Writing – review & editing, Supervision, Methodology, Investigation, Funding acquisition, Formal analysis, Conceptualization.

Declaration of competing interest

The authors declare that they have no known competing financial interests or personal relationships that could have appeared to influence the work reported in this paper.

Data availability

Data will be made available on request.

Appendix A. Supplementary data

Supplementary data to this article can be found online at https://doi.org/10.1016/j.foodres.2024.114119.

References

Abd Alla, S. G., Sen, M., & El-Naggar, A. W. M. (2012). Swelling and mechanical properties of superabsorbent hydrogels based on Tara gum/acrylic acid synthesized by gamma radiation. *Carbohydrate Polymers, 89*, 478–485.

Abedi, E., & Sahari, M. A. (2014). Long-chain polyunsaturated fatty acid sources and evaluation of their nutritional and functional properties. *Food Science & Nutrition, 2* (5), 443–463.

Adachi, M., Kanamori, J., Masuda, T., Yagasaki, K., Kitamura, K., Mikami, B., et al. (2003). Crystal structure of soybean 11S globulin: Glycinin A3B4 homohexamer. *Proceedings of the National Academy of Sciences, 100*(12), 7395–7400.

AOAC, Association of Official Analytical Chemists (1990). Official Method 969.33.

AOAC, Association of Official Analytical Chemists (2001). Official Method 2001.11.

Balaguer, L., Arroyo, R., Jiménez, P., Jiménez, M. D., Villegas, L., Cordero, I., et al. (2011). Forest restoration in a fog oasis: Evidence indicates need for cultural awareness in constructing the reference. *PLoS One, 6*, 1–10.

Bilge, G., Sezer, B., Eseller, K. E., Berberoglu, H., Koksel, H., & Boyaci, I. H. (2016). Ash analysis of flour sample by using laser-induced breakdown spectroscopy. *Spectrochimica Acta Part B: Atomic Spectroscopy, 124*, 74–78.

Borzelleca, J. F., Ladu, B. N., Senti, F. R., & Egle, J. L., Jr (1993). Evaluation of the safety of tara gum as a food ingredient: A review of the literature. *Journal of the American College of Toxicology, 12*(1), 81–89.

Bucar, F., Xiao, J., & Ochensberger, S. (2021). Springer Nature Singapore Pte Ltd.; Xiao J. et al. (eds.), Handbook of Dietary Phytochemicals.

Campos, D., Chirinos, R., Huaraca-Espinoza, P., Aguilar-Galvez, A., García-Ríos, D., Pedreschi, F., et al. (2024). Atmospheric immersion and vacuum impregnation of gallotannins and hydrolysed gallotannins from tara pods (*Caesalpinia spinosa*) mitigate acrylamide and enhances the antioxidant power in potato chips. *Food Chemistry, 436*, Article 137675.

Chambi, F., Chirinos, R., Pedreschi, R., Betalleluz-Pallardel, I., Debaste, F., & Campos, D. (2013). Antioxidant potential of hydrolyzed polyphenolic extracts from tara (*Caesalpinia spinosa*) pods. *Industrial Crops and Products, 47*, 168–175.

Chi, M., Liu, C., Shen, J., Dong, Z., Yang, Z., & Wang, L. (2018). Antibacterial superabsorbent polymers from Tara gum grafted poly (acrylic acid) embedded silver particles. *Polymers, 10*(9), 945.

Chittiboyina, A. G., Ali, Z., Avula, B., Khan, S. I., Mir, T. M., Zhang, J., et al. (2023). Is Baikiain in Tara Flour a Causative Agent for the Adverse Events Associated with the Recalled Frozen French Lentil & Leek Crumbles Food Product? - A Working Hypothesis. *Chemical Research in Toxicology, 36*(6), 818–821.

Cruz Alcedo, G.E. (1999). Production and characterisation of *Prosopis* seed galactomannan. (Doctoral dissertation, ETH Zurich, Permanent link: https://doi.org/10.3929/ethz-a-003838586).

Davies, J., Siebenhandl-Wolff, P., Tranquart, F., Jones, P., & Evans, P. (2022). Gadolinium: Pharmacokinetics and toxicity in humans and laboratory animals following contrast agent administration. *Archives of Toxicology, 96*(2), 403–429.

Desai, S., Prajati, V., Chandarana, C. (2022). Chemistry, Biological Activities, and Uses of Tara Gum. In: Gums, Resins and Latexes of Plant Origin, pp. 265-289.

EFSA Panel on Food Additives and Nutrient Sources added to Food (ANS). Re-evaluation of tara gum (E 417) as a food additive. (2017). *EFSA Journal, 15*(6), e04863.

European Directorate for the Quality of Medicines. Council of Europe. Determination of tannins in herbal drugs (2007). European Pharmacopoeia (6th ed.). France: Strasbourg. p A286.

Firsching, F. H., & Brune, S. N. (1991). Solubility products of the trivalent rare-earth phosphates. *Journal of Chemical & Engineering Data, 36*(1), 93–95.

Gelling, T. (2019). *A chef's guide to gelling, thickening, and emulsifying agents.* Boca Raton: CRC Press.

Geng, P., Sun, J., Zhang, M., Li, X., Harnly, J. M., & Chen, P. (2016). Comprehensive characterization of C-glycosyl flavones in wheat (*Triticum aestivum* L.) germ using UPLC-PDA-ESI/HRMS^n and mass defect filtering. *Journal of Mass Spectrometry, 51* (10), 914–930.

Glicksman, M. (1986). Tara gum. In M. Glicksman (Ed.), *Food hydrocolloids* (vol 3, pp. 185–189). Boca Raton: CRC Press.

Grobbelaar, N., Pollard, J. K., & Steward, F. C. (1955). New soluble nitrogen compounds (amino- and imino-acids and amides) in plants. *Nature, 175*(4460), 703–708.

Hidalgo, M. E., Ingrassia, R., Nielsen, N. S., Porfiri, M. C., Tapia, M. D., & Risso, P. H. (2020). Tara gum–bovine sodium caseinate acid gels: Stabilisation of W/W emulsions. *International Journal of Dairy Technology, 73*(3), 521–531.

Lajolo, F. M., & Genovese, M. I (2002). Nutritional significance of lectins and enzyme inhibitors from legumes. *Journal of Agricultural and Food Chemistry, 50*(22), 6592–6598.

Lee, Y. S., Cho, Y., & Shin, M.-J. (2015). Dietary very long chain saturated fatty acids and metabolic factors: Findings from the Korea National Health and Nutrition Examination Survey 2013. *Clinical Nutrition Research, 4*, 182–189.

Ma, Q., Ren, Y., & Wang, L. (2017). Investigation of antioxidant activity and release kinetics of curcumin from Tara gum/polyvinyl alcohol active film. *Food Hydrocolloids, 70*, 286–292.

Mamone, G., Sciammaro, L., De Caro, S., Di Stasio, L., Siano, F., Picariello, G., et al. (2019). Comparative analysis of protein composition and digestibility of *Ceratonia siliqua* L. and *Prosopis spp.* seed germ flour. *Food Research International, 120*, 188–195.

Mills, E. N., Jenkins, J., Marigheto, N., Belton, P. S., Gunning, A. P., & Morris, V. J. (2002). Allergens of the cupin superfamily. *Biochemical Society Transactions, 30*(Pt 6), 925–929.

Mukherjee, K., Dutta, P., Badwaik, H. R., Saha, A., Das, A., & Giri, T. K. (2023). Food Industry applications of Tara Gum and its modified forms. *Food Hydrocolloids for Health, 3*, Article 100107.

Nitride, C., Picariello, G., Mamone, G., & Ferranti, P. (2017). Proteomics of Hazelnut (*Corylus avellana*). In *Proteomics in Food Science* (pp. 107–125). Academic Press.

Pałasz, A., & Czekaj, P. (2000). Toxicological and cytophysiological aspects of lanthanides action. *Acta Biochimica Polonica, 47*, 1107–1114.

Pedreschi, F., Saavedra, I., Bunger, A., Zuñiga, R. N., Pedreschi, R., Chirinos, R., et al. (2018). Tara pod (*Caesalpinia spinosa*) extract mitigates neo-contaminant formation in Chilean bread preserving their sensory attributes. *LWT, 95*, 116–122.

Pedreschi, F., Matus, J., Bunger, A., Pedreschi, R., Huamán-Castilla, N. L., & Mariotti-Celis, M. S. (2022). Effect of the Integrated Addition of a Red Tara Pods (*Caesalpinia spinosa*) Extract and NaCl over the Neo-Formed Contaminants Content and Sensory Properties of Crackers. *Molecules, 27*, 1020.

Picariello, G., Sciammaro, L., Siano, F., Volpe, M. G., Puppo, M. C., & Mamone, G. (2017). Comparative analysis of C-glycosidic flavonoids from *Prosopis spp*. and *Ceratonia siliqua* seed germ flour. *Food Research International, 99*, 730–738.

Quiroga, I., Regente, M., Pagnussat, L., Maldonado, A., Jorrín, J., & de la Canal, L. (2013). Phosphorylated 11S globulins in sunflower seeds. *Seed Science Research, 23* (3), 199–204.

Rahanitriniaina, D., Artaud, J., Iatrides, M. C., & Gaydou, E. M. (1984). Chemical Composition of tara seed (*Caesalpinia spinosa*, Caesalpiniacee). 1. Fatty acids and sterols. *Revue Francaise des Corps Gras*, *31*(6), 249-252.

Regulation (EC) No 1333/2008 of the European Parliament and of the Council of 16 December 2008 on food additives. OJ L 354, (2008). p. 16-33.

Re-Jiménez, B. L. D., & Amadò, R. (1989). Comparative study of the chemical composition of germ meals from carob, guar and Tara seeds. *Food Hydrocolloids, 3* (2), 149–156.

Rolli, N. M., Karalatti, B. I., & Gadi, S. B. (2015). Metal accumulation profile in roadside soils, grass and Caesalpinia plant leaves: Bioindicators. *Journal of Environmental and Analytical Toxicology, 5*, 319.

Santos, M. B., Dos Santos, C. H., de Carvalho, M. G., de Carvalho, C. W., & Garcia-Rojas, E. E. (2019). Physicochemical, thermal and rheological properties of synthesized carboxymethyl tara gum (*Caesalpinia spinosa*). *International Journal of Biological Macromolecules, 134*, 595–603.

Siano, F., Sciammaro, L., Volpe, M. G., Mamone, G., Puppo, M. C., & Picariello, G. (2018). Integrated analytical methods to characterize lipids from Prosopis spp. and Ceratonia siliqua seed germ flour. *Food Analytical Methods, 11*, 3471–3480.

Siano, F., Mamone, G., Vasca, E., Puppo, M. C., & Picariello, G. (2023). Pasta fortified with *C*-glycosides-rich carob (*Ceratonia siliqua L.*) seed germ flour: Inhibitory activity against carbohydrate digesting enzymes. *Food Research International, 170*, Article 112962.

Siano, F., Sammarco, A. S., Fierro, O., Castaldo, D., Caruso, T., Picariello, G., et al. (2023). Insights into the Structure-Capacity of Food Antioxidant Compounds Assessed Using Coulometry. *Antioxidants, 12*, 1963.

Wu, Y., Ding, W., Jia, L., & He, Q. (2015). The rheological properties of tara gum (*Caesalpinia spinosa*). *Food Chemistry, 168*, 366–371.

Zhang, C., Liu, D., Shi, K., Liu, C., Lyu, K., Chen, J., et al. (2019). Gadolinium accumulation, distribution, chemical forms, and influence on the growth of rice seedlings. *Ecotoxicology and Environmental Safety, 179*, 265–271.